[Palaeontology, Vol. 50, Part 6, 2007, pp. 1519–1529]

EVOLUTION OF HINDLIMB POSTURE IN ARCHOSAURS: LIMB STRESSES IN EXTINCT VERTEBRATES

by TAI KUBO* *and* MICHAEL J. BENTON†

*Department of Earth and Planetary Science, University of Tokyo, Hongo, Tokyo 113-0033, Japan; e-mail: taikubo@eps.s.u-tokyo.ac.jp
†Department of Earth Sciences, University of Bristol, Bristol BS8 1RJ, UK; e-mail: mike.benton@bris.ac.uk

Typescript received 20 February 2006; accepted in revised form 30 November 2006

Abstract: During the Triassic, some 250–200 million years ago, the basal archosaurs showed a transition from sprawling to erect posture. Past studies focused on changes in bone morphology, especially on the joints, as they reorientated from a sprawling to an erect posture. Here we introduce a biomechanical model to estimate the magnitude of femur stress in different postures, in order to determine the most reasonable postures for five basal archosaurs along the line to crocodiliforms (the rhynchosaur *Stenaulorhynchus*, the basal archosaur *Erythrosuchus*, the 'rauisuchian' *Batrachotomus*, the aetosaurs *Desmatosuchus* and *Typothorax*). The results confirm a sprawling posture in basal taxa and an erect posture in derived taxa. Erect posture may have evolved as a strategy to reduce large bending stresses on the limb bone caused by heavy body weights in larger forms.

Key words: limb, posture, stress, archosaurs, Triassic.

THE evolution of locomotion is an important topic in palaeobiology. As direct observations are impossible, several different methods should be applied to cross-check and augment each other; if they broadly agree, then perhaps the correct model has been discovered. The purpose of this paper is to examine the evolution of locomotion in early archosaurs, a well-known case where it has been postulated that posture and gait evolved from the primitive sprawling mode, seen in salamanders and lizards today, to the derived erect mode, seen in birds today.

Archosauria includes birds and crocodylians, as well as the extinct members of the larger clades that include these extant forms, and some basal members, all diagnosed by a number of characters, including the antorbital fenestra, an opening in the side of the skull between the nostril and the eye socket (Benton 2004). The terms 'Archosauria' and 'archosaur' are used here in the broad sense to refer to the clade of proterosuchids and birds, and everything else in between, rather than to indicate the crocodile-bird crown clade. Archosaurs are members of a larger clade, Archosauromorpha, which includes also the bulky herbivorous rhynchosaurs of the Triassic, the long-necked carnivorous prolacertiforms, and other groups (Text-fig. 1). During the Triassic, the basal archosaurs seemingly evolved semi-erect and erect gaits several times, both in the 'crocodile' and in the 'bird' lines of evolution, the Crurotarsi and Ornithodira, respectively (Benton and Clark 1988; Sereno 1991). Erect posture has generally been regarded as in some way advantageous, and a key contributor to the later success of the dinosaurs, pterosaurs and birds (Charig 1972; Bonaparte 1984; Parrish 1986, 1987). These studies were based on the morphology of the pelvis and hindlimb, and it was suggested (Sereno 1991; Gower 2000) that further biomechanical studies are required.

In the Ornithodira, Charig (1972) identified three evolutionary stages: sprawling, semi-erect and erect, each characterized by morphological traits of the pelvis and hind limb bones. Charig (1972) concluded that the upright limb posture was attained by passing through the three stages from sprawling to semi-erect to erect. However, tetrapod posture forms a continuum. Indeed, the alligator may show at least two of these: sprawling and semi-erect. Probably these posture grades are artificial abstractions, but they are still useful as broad descriptors (Gatesy 1991). Erect posture was achieved in ornithodirans by retaining vertical pelvic bones, and modifying the head of the femur to bring this bone close to the vertical, the so-called 'buttress-erect' posture of Benton and Clark (1988). Ornithodirans, notably dinosaurs and birds, also adopted the digitigrade posture, in which the metatarsus is elevated above the substrate.

Erect posture may have arisen more than once in Crurotarsi. Bonaparte (1984) and Parrish (1986, 1987) showed that 'rauisuchians', a poorly defined grouping of large Mid and Late Triassic predatory archosaurs (Gower 1996), attained a vertical hind limb by moving the ilia to a horizontal position and directing the acetabulum almost

 doi: 10.1111/j.1475-4983.2007.00723.x

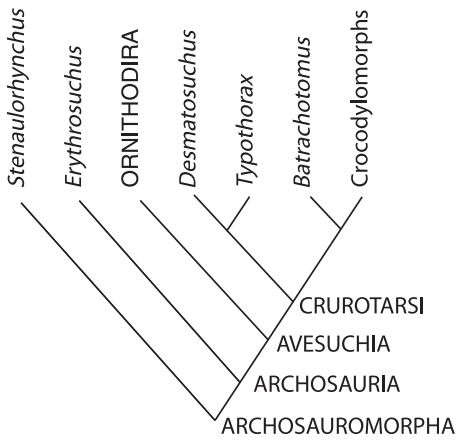

TEXT-FIG. 1. Phylogenetic relationships of the taxa studied based on Benton (2004). The crown-group archosaurs (Avesuchia) are divided into the 'bird/dinosaur line' (Ornithodira) and the 'crocodile line' (Crurotarsi).

ventrally, a configuration termed 'pillar-erect' by Benton and Clark (1988). Rauisuchians are reconstructed as heavy plantigrade tetrapods, and their heavy weight is assumed to have triggered this posture change. Parrish (1986) noted the same phenomenon in aetosaurs. On the other hand, erect-postured basal crocodylomorphs retain vertical ilia, and they have vertical femora whose heads are bent in from the side, similar to the 'buttress-erect' posture of ornithodirans. An erect posture was perhaps plesiomorphic in derived crurotarsans, and the semi-erect posture of modern crocodylians would then be a secondary adaptation for their amphibious habitat, as argued by Parrish (1987). This remarkable observation, that primitively crocodylomorphs were fully erect, is confirmed in the Late Triassic *Terrestrisuchus* (Crush 1984) and the Mid Jurassic *Junggarsuchus sloani* (Clark *et al.* 2004), among other forms. The semi-erect posture was re-acquired in the Jurassic, perhaps as crocodylians adopted more aquatic lifestyles.

The aims of this paper are to investigate how limb-bone stresses vary with posture, and to calculate those stresses in the hindlimbs of a range of basal archosauromorphs in order to test previous assumptions about when and how the postural shifts from sprawling to semi-erect to erect took place.

MATERIAL

Five genera were examined: the rhynchosaurian archosauromorph *Stenaulorhynchus*, the basal archosaur *Erythrosuchus*, the 'rauisuchian' *Batrachotomus*, and the aetosaurs *Typothorax* and *Desmatosuchus*. The first two taxa would conventionally be regarded as sprawlers and the other three as either semi-erect or erect. Most measurements were made directly on the specimens in museum collections in England, Germany and the United States. Where measurements could not be made directly, they were extracted from relevant literature. Some anatomical data (i.e. r_c, $r_{kex}t$, θ_{kext}) were measured from photographed femora. This is detailed in Table 1.

A BIOMECHANICAL MODEL FOR ESTIMATING STRESSES IN THE FEMUR OF EXTINCT ARCHOSAURS

Introduction

Bone stresses constrain the posture and movements of animals. Large mammals mitigate the size-correlated increases of the load on limb bones by adopting more upright postures, and placing their limbs closer to the vector of the ground reaction force (Biewener 1990). In contrast, data from alligators and iguanas show an increase in some limb bone stresses with a more upright posture (Blob and Biewener 1999). In particular, Blob and Biewener (2001) argued that the moment arm of the ground reaction force (GRF) at the ankle was greater in more upright steps for *Iguana* and *Alligator*, leading to higher knee and ankle extensor forces. These higher forces resulted in higher signal intensity of electromyographic patterns during the use of more upright postures (Reilly and Blob 2003). These results suggest that tetrapods generally adopt the posture that minimizes limb bone stresses, except in special cases: for example, alligators may adopt a semi-erect posture for fast walking, even though some stresses increase in this position. Broadly speaking, however, if the bone stresses in various hypothetical postures are calculated for extinct taxa, this may help in reconstruction of their probable posture.

In this study, the biomechanical model of Blob (2001) is applied. This model is based on experiments with extant iguanas and alligators, a limited data set, but perhaps sufficient. The model calculates stresses due to the GRF and knee extensor musculature at the midshaft of the femur in various postures, and adds these stresses to derive the net stress. The model is based on data from tetrapods weighing less than 25·5 kg, and there may be a large error when it is applied to large animals; indeed, Blob (2001) noted that the model tends to overestimate stresses.

Estimation of body mass

As the magnitude of the GRF is assumed to be equal to the body mass in this model, weight estimated for the fossil tetrapods included in the study are needed. Follow-

ing Anderson *et al.* (1985), the body mass estimates are regressed on the mid-shaft circumferences of the humerus (H_c, in mm) and femur (F_c, in mm). The relation between these values and the body mass (M, in g) is expressed as $M = 0{\cdot}084 \times (H_c + F_c)^{2{\cdot}73}$.

There are some weaknesses in using this method. For example, it cannot account for dermal armour in forms such as the aetosaurs. Furthermore, as shown below, morphometric data from the femur are used in the stress calculation, and it might have been better to calculate body mass from measurements of bones other than the femur. Furthermore, tetrapods with non-parasagittal limb posture were not examined in the study of Anderson *et al.* (1985).

Other methods for estimating the body mass of extinct animals, such as measuring the displaced volume of accurate scale models (Colbert 1962) or constructing a 3D computer model and assessing the masses of body slices (Henderson 1999), were not possible here because such models do not exist for these taxa, and the construction of models is beyond the scope of this study. Regardless, methods using actual or mathematical models require assumptions about soft tissue anatomy that can cause substantial error (Motani 2001) and may be no more accurate than the equation of Anderson *et al.* (1985).

Comparison of femur cross-sectional shape and diameter of condyles

For the measurements, the anteroposterior plane is defined as the plane that includes the long axes of both femur and tibia. The dorsoventral plane is the plane that lies perpendicular to the anteroposterior plane and includes the long axis of the femur (Blob 2001). Usually the femur shaft of basal archosaurs is twisted, and the long axes of the proximal and distal ends are not parallel (Parrish 1986). Thus, the long axis of the proximal condyle of the femur is usually not aligned dorsoventrally. The length of the femur is taken as the distance between the midpoints of the articular surfaces at each end of the femur. Calipers were used, and measurements taken to a scale of 0·1 mm.

Forces

The methodological exposition that follows is based substantially on Blob (2001). The GRF and muscular forces both contribute to bone stress; the magnitudes and directions of these forces are needed for the calculations. Postures are represented by an angle between the longitudinal axis of the femur and GRF, where α is defined as the angle between the limb bone and GRF. This angle will be smaller for more upright postures. The GRF can be divided into two components, one along the axis of the bone (GRF_{ax}) and the other transverse to the bone (GRF_{tr}), where $GRF_{ax} = GRF \cos(\alpha)$ and $GRF_{tr} = GRF \sin(\alpha)$.

Bone stresses are calculated for α from 10 to 70 degrees (°) in increments of 5°. The magnitude of the GRF on a single limb is estimated to be equal to the body mass of the animal.

When estimating muscle forces, it is assumed that joints keep a static rotational equilibrium and, as was assumed in some previous studies that estimated limb bone loading (Alexander 1974; Blob and Biewener 2001), the further assumption was made that only muscles that produce a counter force to the rotational moment caused by the GRF are active. Under these assumptions the muscle force (F_m) can be calculated as $F_m = GRF \times R_{GRF}/r_m$, where R_{GRF} is the perpendicular distance (moment arm) between the GRF vector and the joint, and r_m is that of the muscles. The assumption of static rotational equilibrium amounts to ignoring the 'inertial moments' resulting from acceleration and deceleration of the limb segments, but this leads only to minor errors, especially at the more distal joints (Biewener and Full 1992). The model also ignores moments arising from the weight of each limb segment, and the torsional moment exerted by the GRF, although this latter moment could be large in sprawling taxa.

Only muscles that insert distal to the midshaft, such as the knee extensors, may contribute to the maximum bending stress on the femur (Alexander 1974). The magnitude of the knee extensor force is calculated to maintain a static rotational equilibrium with the force exerted by ankle extensors originating from the femur and the GRF as

$$F_{kext} = (GRF \times R_{GRF(knee)} + F_{aext} \times r_{aext(knee)})/r_{kext(knee)}.$$

The knee extensors insert on the proximal end of the tibia, and the width of that bone is matched by the distal width of the femur; thus, half the width of the distal femoral condyle in a dorsoventral direction is assumed as the moment arm at the knee joint for the knee extensors ($r_{kext(knee)}$).

The moment arm of the GRF and other forces counter to the knee extensor muscles (R_{GRF}) is derived from force platform experiments on *Iguana* and *Alligator*. In spite of differences in the body masses of these two animals, R_{GRF} did not differ significantly. It was 1·2 ± 0·6 cm at peak stress at the knee (Blob 2001). However, animals considered here were much larger than those in Blob's experiments, and for these taxa two values, 1·2 cm and 2·4 cm, were used as the values of R_{GRF}. Nevertheless, it is uncertain how values of R_{GRF} respond to increasing body mass;

thus, using 1·2 cm and 2·4 cm may be a potential source of error.

Because ankle extensors also originate from the ventral surface of the distal femur, calculation of the force exerted by the knee extensor (F_{kext}) requires values of the ankle extensor force (F_{aext}) and the length of its moment arm ($r_{aext(knee)}$). The length $r_{aext(knee)}$ is measured as one-half the diameter of the distal femoral condyle in the dorsoventral direction (Text-fig. 2). F_{aext} is calculated as

$$F_{aext} = GRF \times R_{GRF(ankle)}/r_{aext(ankle)}.$$

$r_{aext(ankle)}$ is calculated as the sum of half the length of the distal articular surface of the tibia in the ankle flexion/extension plane and the length of the calcaneal tuber. When the calcaneal tuber is directed laterally, as in *Erythrosuchus* (Gower 1996), the length of the tuber was not considered. Based on experiments with modern iguanas, Blob (2001) found the following empirical formula relating $R_{GRF(ankle)}$ to foot length and to the angle between GRF and femur (α):

$$R_{GRF(ankle)} = \text{Length(foot)} \times (\sin(40{\cdot}361 - 0{\cdot}242\alpha))^2.$$

Calculation of the bone stresses

By convention, tensile stresses are expressed as positive values and compressive stresses as negative values. Stresses are calculated in megapascals (MPa $= 1 \times 10^6$ N/m^2).

At the midshaft of the femur, compressive axial stresses are calculated as

$$\sigma_{ax} = -(F_{kext} \times \cos\theta_{ax} + GRF_{ax})/A,$$

where θ_{ax} is the angle between the long axis of the femur and the knee extensor force, and A is the cross-sectional area at the midshaft of the bone. θ_{ax} is assumed to be 0°, as studies of extant lizards and crocodylians demonstrate that this assumption introduces only a slight potential error. Thus, $\cos\theta_{ax} = 1$, and the above equation can be rewritten as

$$\sigma_{ax} = -(F_{kext} + GRF_{ax})/A.$$

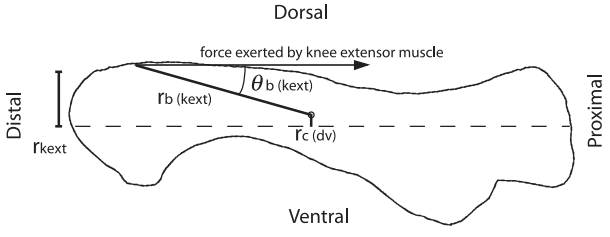

TEXT-FIG. 2. Posterior view of the left femur of *Stenaulorhynchus*, showing various forces and moment arms that are calculated to the bending moment of the knee extensor musculature and bone curvature in a dorsoventral direction.

The bending stresses are calculated as $\sigma_b = M_b \times y/I$, where M_b is the bending moment at the midshaft of the femur, y is the distance from the neutral axis of bending to the bone surface in the plane under consideration, and I is the second moment of area for bending about the neutral axis. Both y and I are calculated in anteroposterior and dorsoventral directions from digitized cross-sections of the midshafts of the femora. To obtain the shape of each cross-section, steel wire was wrapped closely round the midshaft of the femur, and then cut into two parts. These two wires were fixed to 1 mm squared paper and traced. The traced cross-section was then duplicated on the digitized squared sheet used in the computer software (DAN-3) to calculate area, y and I of the cross-section. The ratio of bone to cortex diameter was taken from a femur of the same genus in cases where a femur broken through the middle of the shaft was available (i.e. in *Stenaulorhynchus* and *Erythrosuchus*), but in the other cases bone:cortical ratios were assumed to be the same as in *Alligator mississippiensis* (BMNH unregistered).

Three types of bending moments (σ_b) are considered in this model: the midshaft bending moment produced by the knee extensors (σ_m), the moment due to bone curvature in dorsoventral and anteroposterior directions (σ_{axDV} and σ_{axAP}) and the moment due to the transverse component of the GRF (σ_{tr}).

The midshaft bending moment produced by the knee extensor (M_m) is expressed as

$$M_m = F_{kext} \times r_b \times \sin\theta_b,$$

where r_b is the distance between the point where the muscle force acts on the bone surface and the centroid of the bone, and θ_b is the angle between the line of r_b and the line of muscle force, which is assumed to be parallel to the long axis of the femur for the knee extensor. These measurements are taken from photographed anterior views of the bones.

GRF_{ax} and bone curvature produce the bending moment (M_c), which is calculated in both dorsoventral and anteroposterior directions as

$$M_c = GRF_{ax} \times r_c,$$

where r_c is the distance (in the appropriate plane) between the centroid and the line that connects the midpoints of the distal and proximal articular surfaces.

The moment caused by the transverse component of GRF (M_{tr}) is calculated as

$$M_{tr} = GRF_{tr} \times L/2,$$

where L is the length of the femur.

As a consequence, four bending stresses (σ_b) are calculated; to distinguish each bending stress, four symbols are used, namely σ_m, σ_{tr}, σ_{axDV} and σ_{axAP}, where σ_m is the stress due to the muscle force, σ_{tr} is due to GRF_{tr}, σ_{axDV} is due to bone curvature in the dorsoventral direction, and σ_{axAP} is due to bone curvature in the anteroposterior direction.

The direction of M_{tr} depends on limb movement. Peak femoral bending stress, which is calculated by the addition of σ_{tr} and other stresses, therefore has a range that depends on the direction of σ_{tr}. The stress will be dorsoventrally directed in the case of a sprawling femur that has not rotated around its long axis (i.e. one with its anatomically dorsal surface facing dorsally in absolute terms), but anteroposteriorly directed for a sprawling femur that has rotated, or for a femur that is close to a parasagittal plane. When the direction of σ_{tr} is the same as that of the knee extensors, the net maximum estimate of the bending stress is calculated as the vector sum of stresses in the dorsoventral and anteroposterior directions, perpendicular to each other:

$$\sigma_{bmax} = ((\sigma_m + \sigma_{tr} + \sigma_{axDV})^2 + \sigma_{axAP}{}^2)^{0.5}.$$

When GRF_{tr} is directed in the anteroposterior plane of the bone, the sum of stresses takes a minimum value and is calculated as

$$\sigma_{bmin} = ((\sigma_m + \sigma_{axDV})^2 + \sigma_{tr} + \Sigma^2_{axAP)})^{0.5}.$$

Then the net longitudinal bone stress can be calculated as the sum of σ_{ax} and σ_b. Stresses are calculated for different limb postures by varying α from 10 to 70°, and both σ_{bmin} and σ_{bmax} are used in the calculation in order to bracket the range that σ_b could take. Basic measurements and estimates for each taxon are given in Table 1.

RESULTS

Body masses

Estimated body masses, using the equation of Anderson *et al.* (1985), for the five taxa are: *Stenaulorhynchus* (87 kg), *Erythrosuchus* (1332 kg), *Batrachotomus* (247 kg), *Desmatosuchus* (284 kg) and *Typothorax* (68 kg).

Outline shape of the femur

Femur cross-sectional shapes in most specimens are flattened in an anteroposterior direction. The ratio of the midshaft dorsoventral diameter to the midshaft anteroposterior diameter is 1·12 in *Stenaulorhynchus*, 0·77 in *Erythrosuchus*, 0·69 in *Desmatosuchus*, 0·54 in *Batrachotomus* and 0·97 in *Typothorax* (Text-fig. 3). These values may be compared with averages of 0·88 for 16 modern crocodylian species and 0·90 for 25 modern iguana species (Blob 2000).

Stress calculations from the biomechanical model

Estimated values of femur stresses using two values of R_{GRF} for specific postures are reported in Table 2. When 2·4 cm was adopted as the value of R_{GRF} instead of 1·2 cm, the magnitudes of both compressive and tensile stresses increased to some extent in all taxa, but actually by less than 35 per cent. Moreover, patterns of stress change (increasing or decreasing with larger α values) are the same for the same genus regardless of R_{GRF} values. This suggests that the assumed value for R_{GRF} does not greatly influence the results and, for convenience, stress values that are obtained with the smaller value of R_{GRF} will mainly be used below.

Posture-related femoral stresses show a wide range between maximum and minimum values in some genera (Text-fig. 4; Table 2). The estimates of minimum and maximum stress tend to converge at lower α values (i.e. at more upright postures) for all species. This happens because the transverse stress associated with GRF, which accounts for the discrepancy between maximum and minimum estimates, is lower in upright postures. The differ-

TABLE 1. Anatomical data from basal archosaur specimens used in the biomechanical model.

Taxon	Mass (kg)	r_{kext} (mm)	r_{aext} (ankle) (mm)	Femur length (mm)	Femur area (mm^2)	y_{dv} (mm)	I_{dv} (mm^4)	r_c (dv) (mm)	y_{ap} (mm)	I_{ap} (mm^4)	r_c (ap) (mm)	Foot length (mm)	r_{kext} (shaft) (mm)	θ_{kext} (shaft) (°)	Literature
Stenaulorhynchus stockleyi	86·7	18·6	14·8	172	258	14	15 400	−3·8	13	18 600	−7·6	222	63·4	15·8	
Erythrosuchus africanus	1332·4	63·5	48	494	1919	27	602 800	5·3	34	991 000	−18·9	282·8	249·5	16·7	Cruickshank (1978)
Batrachotomus kupferzellensis	246·7	22·4	64·4	464	1256	14·5	79 800	−11·6	29	292 400	−27·6	334·8	205·8	6·8	
Desmatosuchus haplocerus	284·4	27·9	67·9	370	1435	20·5	176 300	14·5	25·5	342 500	−21·8	281·4	132·6	17·3	Long and Murray (1995)
Typothorax meadei	67·8	22·8	38	232	297·9	15·4	23 900	−6·0	15·4	23 700	−10·2	165	103·7	13·2	Sawin (1947)

Abbreviations: r_{kext}, moment arm of knee extensor; r_{aext}(ankle), moment arm of ankle extensor about ankle; dv, dorsoventral direction; ap, anteroposterior direction; y, distance from neutral axis to bone surface; I, second moment of area; r_c, moment arm due to bone curvature; r_{kext} (shaft), knee extensor moment arm about midshaft centroid; θ_{kext}(shaft), angle between extensor force and r_{kext} (shaft).

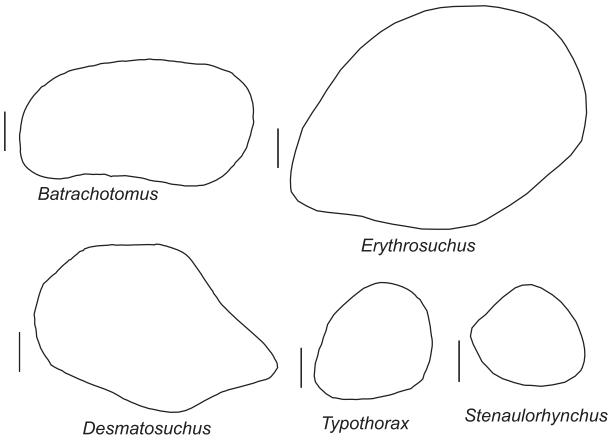

TEXT-FIG. 3. Cross-sectional shapes of the mid-shafts of the femora of the taxa studied. All scale bars represent 10 mm.

ences between maximum and minimum values at $\alpha = 70°$, for example, are 11 MPa for *Typothorax* and 72 MPa for *Erythrosuchus*, and these fall to 8 MPa for *Typothorax* and 35 MPa for *Erythrosuchus* at $\alpha = 10°$. As a consequence, in the tensile stress of *Stenaulorhynchus* and the compressive stress of *Erythrosuchus*, the maximum and minimum stress estimates have slopes of opposite sign, when plotted against α.

Estimates of femur stresses in *Stenaulorhynchus*, *Erythrosuchus* and *Batrachotomus* are high. The maximum estimate of compressive stress for *Erythrosuchus* exceeds −194 MPa at $\alpha = 70°$, and even minimum estimates of the compressive stress range from −116 (at $\alpha = 35°$) to −128 MPa (at $\alpha = 10°$). These maximum values exceed the values of femur stress reported from various extant mammals. The minimum estimate for *Erythrosuchus* is barely comparable with the stresses in running mammals (Alexander *et al.* 1979). For *Stenaulorhynchus*, the maximum estimate of compressive stress approaches −119 MPa at $\alpha = 35°$, and the minimum estimates of the compressive stress range from −71 (at $\alpha = 70°$) to −105 MPa (at $\alpha = 10°$). Also, maximum stress estimates of *Batrachotomus* exceed 100 MPa when the value of α is close to 70°, though stresses are low (< 50 MPa) with small α. These values may be over-estimated, as Blob (2001) noted, because his model is likely to derive higher values than are found in experiments, especially when the value of α is small. Among the other genera examined, the highest maximum stress does not exceed 80 MPa for any value of α.

Each of the five taxa shows a different pattern of variation in stresses with changes in posture. In *Stenaulorhynchus*, minimum tensile and compressive stresses increase with a more upright posture (as α approaches 10°). However, the maximum compressive stress has its highest value at $\alpha = 35°$, and the maximum tensile stress decreases with more upright posture. The range from $\alpha = 70°$ to $\alpha = 35°$ is only about 6 MPa (5% of the peak value) in maximum compressive stress. The increase in maximum tensile stress from $\alpha = 10°$ (upright) to $\alpha = 70°$ (sprawling), and its percentage to the peak stress values, are 22 MPa and 24%. The increase in stresses from $\alpha = 70°$ (sprawling) to $\alpha = 10°$ (upright) are 8 MPa (13%) in minimum tensile stress, and 34 MPa (32%) in minimum compressive stress.

In *Erythrosuchus*, maximum compressive and tensile stresses decrease with a more upright posture. From $\alpha = 10°$ (upright) to $\alpha = 70°$ (sprawling), stresses range through 67 MPa (39%) in maximum tensile stress,

TABLE 2. Minimum and maximum estimates of peak tensile and compressive stresses (in MPa) calculated for fossil specimens in different postures. Absolute stress magnitude differences between $\alpha = 10°$ and 70° are reported. Stresses are calculated using two values for the moment arm of GRF. Lower values of the angle (α) correspond to more upright posture

		R_{GRF} = 1·2 cm								R_{GRF} = 2·4 cm							
		10°		40°		70°		Stress |70° − 10°|		10°		40°		70°		Stress |70° − 10°|	
Angle (α) Specimen		Max.	Min.	Max.	Min.	Max.	Min.	Max.	Min.	Max.	Min.	Max.	Min.	Max.	Min.	Max.	Min.
Stenaulorhynchus	Tensile	69	57	83	48	90	50	21	7	75	64	90	53	97	53	22	11
	Compressive	−117	−105	−118	−83	−112	−71	5	34	−127	−116	−129	−93	−123	−80	4	36
Erythrosuchus	Tensile	107	82	151	82	174	102	67	20	113	88	157	87	180	104	67	16
	Compressive	−153	−128	−185	−116	−194	−122	41	6	−162	−137	−194	−123	−203	−127	41	20
Batrachotomus	Tensile	33	15	77	30	105	48	72	33	38	20	82	32	110	49	72	29
	Compressive	−47	−29	−87	−40	−112	−55	65	26	−53	−35	−94	−44	−119	−58	66	23
Desmatosuchus	Tensile	35	24	57	27	69	35	34	11	40	29	62	30	74	37	34	8
	Compressive	−47	−36	−66	−36	−75	−41	28	5	−53	−42	−72	−41	−81	−44	28	2
Typothorax	Tensile	21	13	42	27	55	44	34	31	26	17	46	29	59	44	33	27
	Compressive	−35	−27	−52	−38	−62	−51	27	24	−42	−33	−59	−42	−68	−53	26	20

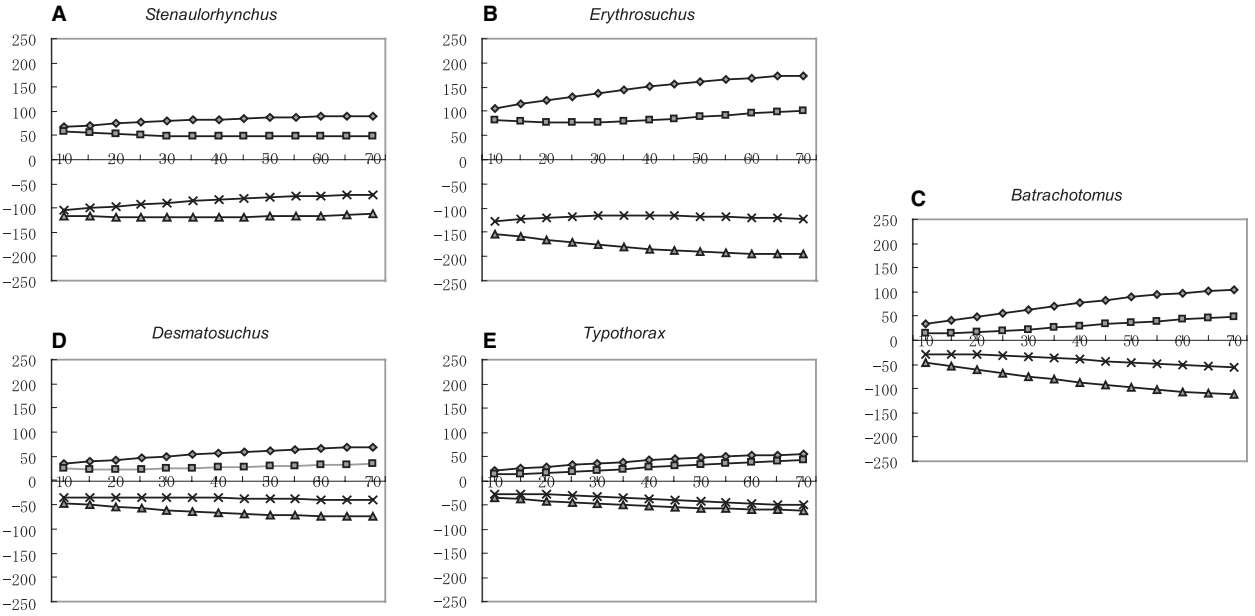

TEXT-FIG. 4. Plots of posture-related changes in femoral stresses calculated for biomechanical models of five archosauromorphs using 1·2 cm as the value of R_{GRF}. The *x*-axis represents values of α (the angle between the ground reaction force and the femur). Upright postures are reflected in smaller values of α. Lines indicate the maximum tensile stress, minimum tensile stress, minimum compressive stress and maximum compressive stress from top to bottom. Graphs of posture-related changes for, A, the rhynchosaur *Stenaulorhynchus*; B, the basal archosaur *Erythrosuchus*; C, the 'rausiuchian' *Batrachotomus*; D, the aetosaur *Desmatosuchus*; and E, the aetosaur *Typothorax*.

41 MPa (21%) in maximum compressive stress. However, the minimum compressive stress has its lowest value at $\alpha = 35°$ and the minimum tensile stress has its lowest value at $\alpha = 25°$. The range from $\alpha = 70°$ to $\alpha = 25°$ is about 25 MPa (24% of the peak value at $\alpha = 70°$) in minimum tensile stress, and the range from $\alpha = 10°$ to $\alpha = 35°$ in the minimum compressive stress is only 13 MPa (10% of the peak value at $\alpha = 10°$).

The other three genera show a decrease in all stresses with more upright posture. The patterns of these three are similar: the percentages of change in maximum tensile stresses, minimum tensile stresses, maximum compressive stresses and minimum compressive stresses from $\alpha = 10°$ (upright) to $\alpha = 70°$ (sprawling) for each genus are, respectively, 68% (72 MPa), 68% (33 MPa), 58% (65 MPa) and 48% (26 MPa) for *Batrachotomus*, 61% (33 MPa), 70% (31 MPa), 42% (26 MPa) and 47% (24 MPa) for *Typothorax*, and 49% (34 MPa), 30% (11 MPa), 38% (28 MPa) and 11% (5 MPa) for *Desmatosuchus*.

The calculated compressive stresses (minimum and maximum) in Table 2 are larger than the corresponding tension values because axial compression is being superimposed on bending stresses that cause equal amounts of tension and compression. Note also that torsional stresses will always act on the femur during locomotion, but they are not accounted for in the model.

DISCUSSION

Shape of the midshaft cross-section and proportions of the femur

Besides *Stenaulorhynchus* and *Typothorax*, the femora studied show a flattened cross-sectional shape in the anteroposterior direction. If constructed from the same amount of bone material, an asymmetrical shape is not as resistant to torsional stresses as a symmetrical shape (Swartz *et al.* 1992). Quantitative kinematic studies suggest that most modern saurians rotate their femora during locomotion (Brinkman 1980; Blob and Biewener 1999). In modern crocodylians and iguanas, significant torsional stresses are caused by axial rotation of the femur during locomotion, and torsional stress predominates over bending stress, which is the main stress in the femora of modern mammals (Blob and Biewener 1999). The cross-sectional shapes of the femora of *Erythrosuchus*, *Desmatosuchus* and *Batrachotomus* are markedly flattened compared with those of modern iguanas and crocodylians. This might suggest that these archosaurs did not employ much rotation of the femur during leg motion, which is common in modern sprawlers. Decrease in the torsion of the basal archosaur femur shaft, measured by the angle between the longitudinal axes of the proximal and distal ends, also indicates locomotion with less femo-

ral rotation than in modern forms (Parrish 1986). The angle between the two ends of the femur was about 30° in the specimen of *Stenaulorhynchus*, about 20° in *Erythrosuchus* and about 0° in *Batrachotomus*.

Nevertheless, the femora of *Desmatosuchus*, *Batrachotomus* and especially *Erythrosuchus* have a prominent fourth trochanter, which clearly points to rotation of the femur during contraction of the M. caudofemoralis. Thus, the strictly mechanical interpretation should be treated with caution because mechanics is not the only functional demand that affects bone morphology. Also, under different locomotor systems, the same morphology may have different mechanical implications.

Posture change in basal archosaurs inferred from the biomechanical model

Estimated values of stresses in femora show a relatively wide range between maxima and minima in *Stenaulorhynchus*, *Erythrosuchus* and *Batrachotomus*. The magnitude of the difference between maximum and minimum values depends mainly on the difference between the two values of the second moment of area, I_{dv} and I_{ap}. Thus, flattening the cross-sectional shape of the femur enlarges the difference between maximum and minimum estimates, as it increases the difference. Femoral stresses are at a maximum when the bending stresses due to the GRF and the knee extensor muscles work in the same plane. In contrast, when these two forces are perpendicular to each other, the femur stresses are at a minimum. Blob (2001, p. 34) mentioned that 'If the femur does not rotate about its long axis, then bending stresses induced by the knee extensors and GRF will sum in the same plane.' Thus, minimum stress estimates may be more reliable for sprawlers as they used femoral rotation.

Apart from *Typothorax* and *Desmatosuchus*, maximum stresses in the femora of basal archosaurs appear to have been relatively high compared with modern animals. Estimates of the maximum stress in mammal leg bones range from 50 to 150 MPa (Alexander *et al.* 1979). The reported ultimate bending strength of the femur in mammals is 90–247 MPa, in reptiles 174–316 MPa and in birds 96–311 MPa (Erickson *et al.* 2002). The highest stresses calculated for *Stenaulorhynchus* (−118 MPa when R_{GRF} is 1·2 cm and −129 MPa when R_{GRF} is 2·4 cm) and *Batrachotomus* [−112 MPa ($R_{GRF} = 1{\cdot}2$ cm) and −119 MPa ($R_{GRF} = 2{\cdot}4$ cm)] are comparable with stresses reported in dog, kangaroo or buffalo during strenuous activities. The highest maximum stresses of *Erythrosuchus* [−194 MPa ($R_{GRF} = 1{\cdot}2$ cm) and −203 MPa ($R_{GRF} = 2{\cdot}4$ cm)], which occurred in the sprawling posture (at $\alpha = 70°$), are much higher than stresses experienced by modern mammals and even exceed the stress that causes bone fracture for some taxa. Even if bones of *Erythrosuchus* were as robust as those of the toughest living reptiles, the safety factor (the value derived from the ultimate strength of the bone divided by stress loaded on the bone) would have been only 1·56 (316/203). This value is low compared with safety factors for mammals and birds, which vary between 1·4 and 4·3, or for living reptiles, which vary from 5·5 to 10·8 (Blob and Biewener 1999). In the upright posture, when $\alpha = 10°$, maximum estimates of bending stress decrease for *Erythrosuchus* [−153 MPa ($R_{GRF} = 1{\cdot}2$ cm) and −162 MPa ($R_{GRF} = 2{\cdot}4$ cm)].

It is worth considering whether such low safety factors are likely. Note that for *Erythrosuchus* the situation may seem even worse if posture is considered. Even in a near-erect posture, femoral stresses seem remarkably high, and safety factors dangerously low. These values would be even more extreme if *Erythrosuchus* were a sprawler, as traditionally assumed (Parrish 1986). Given the known tendency of the model to over-estimate stresses sometimes, it could be that the very high stress values and low safety factors for *Erythrosuchus* indicate an anomaly of the method, rather than being realistic estimates.

Did the basal archosaurs evolve an erect posture to avoid bending stresses caused by evolving large size, or did they become erect first and larger later? Large mammals have a more upright posture than small mammals to prevent high bending stresses in their limbs (Biewener 1989). It is perhaps plausible that archosaurs could not moderate stress by rotating the femur and so, as they became larger, increased bending stress forced them to take an upright posture. Or, alternatively, basal archosaurs that evolved an upright posture could have become larger and, as large body size was beneficial, they may have become even more upright. The former hypothesis agrees with the conclusion of the morphological study by Bonaparte (1984) that proposed heavy body weight as the cause of erect posture in rauisuchians. However, it should be noted that the erect posture of basal mammals and dinosaurs evolved in small ancestors.

The estimated stress pattern may indicate posture. *Typothorax* shows an increase in all stresses with larger α (a more sprawling posture). In *Batrachotomus* minimum stresses decrease from $\alpha = 5$–$10°$ and minimum stresses decrease from $\alpha = 5$–20 or $25°$ in *Desmatosuchus*. However, the decreases are very slight, and generally the stresses in these two taxa increase with a more sprawling posture. The results for these three taxa probably indicate an erect posture. It should be noted that the same criterion would predict an erect posture for *Alligator* (Blob 2001), so the intermediate posture between sprawling and erect might be recognized as erect. The two most basal archosauromorphs studied here, *Erythrosuchus* and *Stenaulorhynchus*, show a more complex pattern. In *Erythrosuchus*, both maximum stresses increase with a more

sprawling posture, the minimum stresses show the lowest peak at $\alpha = 25°$ (tensile) and $\alpha = 35°$ (compressive), the minimum tensile stress is 15 MPa higher at $\alpha = 70°$ (sprawling) than at $\alpha = 10°$ (erect), but the minimum compressive stress is slightly lower (6 MPa) at $\alpha = 70°$ (sprawling) than at $\alpha = 10°$ (erect). If the stresses took intermediate values between the maximum and minimum estimates, both tensile and compressive tresses in *Erythrosuchus* were very likely to increase with a more sprawling posture. Relatively large estimated stresses compared with the other studied taxa indicate that stress may have been an important factor in restricting the posture of *Erythrosuchus*. If *Erythrosuchus* used axial rotation of its femur during locomotion, the magnitudes of the stresses are probably close to minimum estimates (Blob 2001), which do not vary with posture and make it difficult to infer their limb posture. On the other hand, without femur rotation, a more erect posture is safer for *Erythrosuchus*. In *Stenaulorhynchus*, the maximum tensile stress increases by 22 MPa and the minimum tensile stress decreases slightly (7 MPa) from $\alpha = 10°$ (erect) to $\alpha = 70°$ (sprawling). The maximum compressive stress shows its highest peak at $\alpha = 35°$ and the stress is slightly lower (4 MPa) at $\alpha = 70°$ (sprawling) than at $\alpha = 10°$ (erect), and the minimum compressive stress decreases to 34 MPa from $\alpha = 10°$ to $\alpha = 70°$. The relatively large σ_{ax} of *Stenaulorhynchus* caused the opposite effect, an increase in tensile stress and decrease in compressive stress. Change in the compressive stress is steeper than that of the tensile stress and the absolute magnitude of the compressive stress is larger than the tensile stress, so the tensile stress may restrict posture more than the compressive stress does for *Stenaulorhynchus*. If the femur of *Stenaulorhynchus* rotated during locomotion, both tensile and compressive stress might have decreased with a more sprawling posture as the stresses probably take a value close to the minimum estimate. This result might indicate a sprawling posture for *Stenaulorhynchus*, but the indication is not very strong. At least, our estimated stresses suggest that *Stenaulorhynchus* is most adapted for a sprawling posture among the animals investigated here. Unlike other studied taxa, an erect posture would not help to reduce femur stresses for *Stenaulorhynchus*. The results of this biomechanical test support the traditional story, based on morphological evidence, that archosaurs evolved from a sprawling to an erect posture during the Triassic.

Which factor determines whether femur stress increases or decreases along with α in this biomechanical model? Among the five stresses added to calculate net stress, namely σ_m, σ_{tr}, σ_{axDV}, σ_{axAP} and σ_{ax}, the compressive axial stress (σ_{ax}) and bending stresses due to bone curvature (σ_{axDV} and σ_{axAP}) are much smaller than other two stresses and have limited effects. Of the remaining two stresses, the bending stress due to the knee extensor muscle (σ_m) decreases with larger α value (more erect posture), whereas the bending stress caused by the transverse components of GRF (σ_{tr}) increases with larger α value. Thus the relative magnitude of these two stresses virtually determines the tendency of net stress: σ_{tr} is due to the bending moment of GRF_{tr} at the femur; σ_m is due to the bending moment of the force of knee extensor (F_{kext}). F_{kext} can be divided into two forces that counter GRF and the force of the ankle extensor at the knee. Of these two, the force of the ankle extensor is relatively large, especially for animals that show a relatively large σ_m compared with σ_{tr}. Thus, very roughly speaking, the magnitude of the ankle extensor force determines the tendency of net femur stress in this model. This force is proportional to GRF and foot length and inversely proportional to the anteroposterior length of the calcaneal tuber and half the distal condyle of the tibia ($r_{aext(ankle)}$). If this force is large, net femur stress decreases with larger α value (more sprawling posture), which may indicate a sprawling posture. Therefore, the posteriorly directed calcaneal tuber is significant in this model. Among the five taxa, *Stenaulorhynchus* and *Erythrosuchus* possess only modest laterally projected calcaneal tubers (Hughes 1968), much smaller than in the later, apparently more erect, taxa. Considering that the tuber helps movement of the foot in the sagittal plane, it is interesting that in both mammalian and crocodilian lineages, the calcaneal tuber first appeared at about the time when both lineages are thought to have evolved erect posture.

Past studies may have simplified posture changes too much by categorizing postures as sprawling, semi-erect and erect, and assuming that animals in a given category are uniform in their locomotor abilities. Kinematic studies of extant tetrapods show that there are many variations in locomotion among 'sprawling' amphibians and reptiles (Ashley-Ross 1994; Irschick and Jayne 1999; Russell and Bels 2001), and also small mammals are 'semi-erect' in that they abduct their femora during locomotion (Jenkins 1971). Applying this categorization to extinct animals gives the impression that posture change happened in a very short period. It was thought that the erect posture evolved in multiple lineages of archosaurs contemporaneously (once or twice in crurotarsans, once in ornithodirans), probably driven by ecological pressures. If the limb structures that do not increase stresses in erect posture had been acquired gradually in more basal taxa, contemporaneous evolutionary change could have occurred more easily.

CONCLUSION

The results of the biomechanical calculations indicate that basal archosaurs changed their posture from sprawling to

erect, which is consistent with the conclusions of past morphological studies. All three derived archosaurian taxa examined here, *Batrachotomus*, *Desmatosuchus* and *Typothorax*, show decreases in femur stress with a more upright posture. The most basal taxon, *Stenaulorhynchus*, shows a decrease in the compressive stress of the femur with a more sprawling posture and its tensile stress does not increase with a more sprawling posture as much as others. Stress changes in *Erythrosuchus*, which is positioned phylogenetically between these two groups, are intermediate. The flattened cross-sectional shape of the femur in archosaurs indicates that they probably employed less femur rotation during limb movement, which reduces stresses on the limb bones of modern sprawlers. As a consequence, in the crocodylian lineage, an erect posture might have evolved as an adaptation to mitigate large stresses caused by heavy body weight.

Acknowledgements. We acknowledge the critical review and advice of R. W. Blob, and we thank Corwin Sullivan and an anonymous reviewer for their detailed and helpful comments. TK thanks his parents for financial support, Simon Braddy for useful advice and the Palaeontological Association for a Sylvester-Bradley award. We thank the following for permission to work in their collections and hospitality: S. D. Chapman, the Natural History Museum, London; A. Matzke, Paläontologisches Museum, Tübingen; R. R. Schoch, Staatliches Museum für Naturkunde, Stuttgart; and P. A. Holroyd, University of California Museum of Palaeontology. This study formed part of TK's work for his MSc in Palaeobiology at Bristol University.

REFERENCES

ALEXANDER, R. M. 1974. The mechanics of jumping by a dog (*Canis familiaris*). *Journal of Zoology*, **173**, 549–573.

—— MALOIY, G. M. O., HUNTER, B., JAYES, A. S. and NTURIBI, J. 1979. Mechanical stresses in fast locomotion of buffalo (*Syncerus caffer*) and elephant (*Loxodonta africana*). *Journal of Zoology*, **189**, 135–144.

ANDERSON, J. F., HALL-MARTIN, A. and RUSSELL, D. A. 1985. Long bone circumference and weight in mammals, birds and dinosaurs. *Journal of Zoology*, **207**, 53–61.

ASHLEY-ROSS, M. A. 1994. Hindlimb kinematics during terrestrial locomotion in a salamander (*Dicamptodon tenebrosus*). *Journal of Experimental Biology*, **193**, 255–283.

BENTON, M. J. 2004. Origin and relationships of Dinosauria. 7–19. *In* WEISHAMPEL, D. B., DODSON, P. and OSMÓLSKA, H. (eds). *The Dinosauria*. Second edition. University of California Press, Berkeley, CA, 861 pp.

—— and CLARK, J. 1988. Archosaur phylogeny and the relationships of the Crocodylia. 295–338. *In* BENTON, M. J. (ed.). *The phylogeny and classification of the tetrapods*. Systematics Association, Special Volume, **35A**, 377 pp.

BIEWENER, A. A. 1989. Scaling body support in mammals: limb posture and muscle mechanics. *Science*, **245**, 45–48.

—— 1990. Biomechanics of mammalian terrestrial locomotion. *Science*, **250**, 1097–1103.

—— and FULL, R. J. 1992. Force platform and kinematic analysis. 45–73. *In* BIEWENER, A. A. (ed.). *Biomechanics of structures and systems: a practical approach*. Oxford University Press, New York, NY, 310 pp.

BLOB, R. W. 2000. Interspecific scaling of the hindlimb skeleton in lizards, crocodilians, felids and canids: does limb bone shape correlate with limb posture? *Journal of Zoology*, **250**, 507–531.

—— 2001. Evolution of hindlimb posture in nonmammalian therapsids: biomechanical tests of paleontological hypotheses. *Paleobiology*, **27**, 14–38.

—— and BIEWENER, A. A. 1999. *In vivo* locomotor strain in the hindlimb bones of *Alligator mississippiensis* and *Iguana iguana*: implication for the evolution of limb bone safety factor and non-sprawling limb posture. *Journal of Experimental Biology*, **202**, 1023–1046.

—— —— 2001. Mechanics of limb bone loading during terrestrial locomotion in the green iguana (*Iguana iguana*) and American alligator (*Alligator mississippiensis*). *Journal of Experimental Biology*, **204**, 1099–1122.

BONAPARTE, J. F. 1984. Locomotion in rauisuchid thecodonts. *Journal of Vertebrate Paleontology*, **3**, 210–218.

BRINKMAN, D. 1980. The hind limb step cycle of *Caiman sclerops* and the mechanics of the crocodile tarsus and metatarsus. *Canadian Journal of Zoology*, **58**, 2187–2200.

CHARIG, A. J. 1972. The evolution of the archosaur pelvis and hindlimb: an explanation in functional terms. 121–151. *In* JOYSEY, K. A. and KEMP, T. S. (eds). *Studies in vertebrate evolution.* Oliver and Boyd, Edinburgh, 284 pp.

CLARK, J. M., XU, X., FOSTER, C. A. and WANG, Y. 2004. A Middle Jurassic 'sphenosuchian' from China and the origin of the crocodylian skull. *Nature*, **430**, 1021–1024.

COLBERT, E. H. 1962. The weights of dinosaurs. *American Museum Novitates*, **2076**, 1–16.

CRUICKSHANK, A. R. I. 1978. The pes of *Erythrosuchus africanus* Broom. *Zoological Journal of the Linnean Society*, **62**, 161–177.

CRUSH, P. 1984. A late Upper Triassic sphenosuchid crocodile from Wales. *Palaeontology*, **27**, 133–157.

ERICKSON, G. M., CATANESE, J. III and KEAVENY, T. M. 2002. Evolution of the biomechanical material properties of the femur. *Anatomical Record*, **268**, 115–124.

GATESY, S. M. 1991. Hind limb movements of the American alligator (*Alligator mississippiensis*) and postural grades. *Journal of Zoology*, **224**, 577–588.

GOWER, D. J. 1996. The tarsus of erythrosuchid archosaurs, and implications for early diapsid phylogeny. *Zoological Journal of the Linnean Society*, **116**, 347–375.

—— 2000. Rauischian archosaurs (Reptilia, Diapsida): an overview. *Neues Jahrbuch für Geologie und Paläontologie, Abhandlungen*, **218**, 447–488.

HENDERSON, D. M. 1999. Estimating the masses and centers of mass of extinct animals by 3-D mathematical slicing. *Paleobiology*, **25**, 88–106.

HUGHES, B. 1968. The tarsus of rhynchocephalian reptiles. *Journal of Zoology*, **156**, 457–481.

IRSCHICK, D. J. and JAYNE, B. C. 1999. Comparative three-dimensional kinematics of the hindlimb for high-speed bipedal and quadrapedal locomotion of lizards. *Journal of Experimental Biology*, **202**, 1047–1065.

JENKINS, F. A. 1971. Limb posture and locomotion in the Virginia opossum (*Didelphis marsupialis*) and in other non-cursorial mammals. *Journal of Zoology*, **165**, 303–315.

LONG, R. A. and MURRAY, P. A. 1995. Late Triassic (Carnian and Norian) tetrapods from the southwestern United States. *Bulletin of the New Mexico Museum of Natural History and Science*, **4**, 1–254.

MOTANI, R. 2001. Estimating body mass from silhouettes: testing the assumption of elliptical body cross-sections. *Paleobiology*, **27**, 735–750.

PARRISH, J. M. 1986. Locomotor adaptations in the hindlimb and pelvis of the Thecodontia. *Hunteria*, **1**, 1–36.

—— 1987. The origin of crocodilian locomotion. *Paleobiology*, **13**, 396–414.

REILLY, S. M. and BLOB, R. W. 2003. Motor control of locomotor hindlimb posture in the American alligator (*Alligator mississippiensis*). *Journal of Experimental Biology*, **206**, 4327–4340.

RUSSELL, A. P. and BELS, V. 2001. Biomechanics and kinematics of limb-based locomotion in lizards: review, synthesis and prospectus. *Comparative Biochemistry and Physiology, Part A*, **131**, 89–112.

SAWIN, H. J. 1947. The pseudosuchian reptile *Typothorax meadei*. *Journal of Paleontology*, **21**, 201–238.

SERENO, P. C. 1991. Basal archosaurs: phylogenetic relationships and functional implications. *Journal of Vertebrate Paleontology*, **11**, 1–53.

SWARTZ, S. M., BENNETT, M. B. and CARRIER, D. R. 1992. Wing bone stresses in free flying bats and the evolution of skeletal design for flight. *Nature*, **359**, 726–729.